



**HAL**  
open science

# Thermophoretic Hydromagnetic Dissipative Heat and Mass Transfer with Lateral Mass Flux, Heat Source, Ohmic Heating and Thermal Conductivity Effects: Network Simulation Numerical Study

Joaquín Zueco, O. Anwar Bég, H.S. Takhar, V.R. Prasad

► **To cite this version:**

Joaquín Zueco, O. Anwar Bég, H.S. Takhar, V.R. Prasad. Thermophoretic Hydromagnetic Dissipative Heat and Mass Transfer with Lateral Mass Flux, Heat Source, Ohmic Heating and Thermal Conductivity Effects: Network Simulation Numerical Study. Applied Thermal Engineering, 2009, 29 (14-15), pp.2808. 10.1016/j.applthermaleng.2009.01.015 . hal-00556846

**HAL Id: hal-00556846**

**<https://hal.science/hal-00556846>**

Submitted on 18 Jan 2011

**HAL** is a multi-disciplinary open access archive for the deposit and dissemination of scientific research documents, whether they are published or not. The documents may come from teaching and research institutions in France or abroad, or from public or private research centers.

L'archive ouverte pluridisciplinaire **HAL**, est destinée au dépôt et à la diffusion de documents scientifiques de niveau recherche, publiés ou non, émanant des établissements d'enseignement et de recherche français ou étrangers, des laboratoires publics ou privés.

## Accepted Manuscript

Thermophoretic Hydromagnetic Dissipative Heat and Mass Transfer with Lateral Mass Flux, Heat Source, Ohmic Heating and Thermal Conductivity Effects: Network Simulation Numerical Study

Joaquín Zueco, O. Anwar Bég, H.S. Takhar, V.R. Prasad

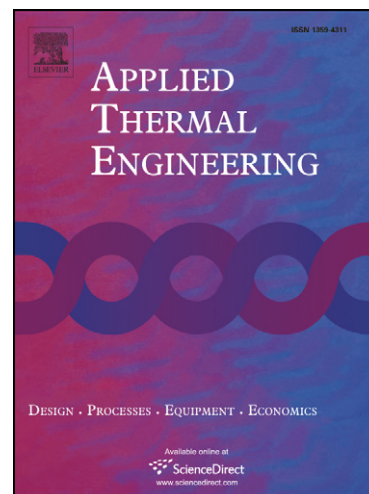
PII: S1359-4311(09)00041-6  
DOI: [10.1016/j.applthermaleng.2009.01.015](https://doi.org/10.1016/j.applthermaleng.2009.01.015)  
Reference: ATE 2730

To appear in: *Applied Thermal Engineering*

Received Date: 7 September 2007  
Accepted Date: 31 January 2009

Please cite this article as: J. Zueco, O. Anwar Bég, H.S. Takhar, V.R. Prasad, Thermophoretic Hydromagnetic Dissipative Heat and Mass Transfer with Lateral Mass Flux, Heat Source, Ohmic Heating and Thermal Conductivity Effects: Network Simulation Numerical Study, *Applied Thermal Engineering* (2009), doi: [10.1016/j.applthermaleng.2009.01.015](https://doi.org/10.1016/j.applthermaleng.2009.01.015)

This is a PDF file of an unedited manuscript that has been accepted for publication. As a service to our customers we are providing this early version of the manuscript. The manuscript will undergo copyediting, typesetting, and review of the resulting proof before it is published in its final form. Please note that during the production process errors may be discovered which could affect the content, and all legal disclaimers that apply to the journal pertain.



# Thermophoretic Hydromagnetic Dissipative Heat and Mass Transfer with Lateral Mass Flux, Heat Source, Ohmic Heating and Thermal Conductivity Effects: Network Simulation Numerical Study

**Joaquín Zueco \***

Professor, ETS Ingenieros Industriales Campus Muralla del Mar, Departamento de Ingeniería Térmica y Fluidos, Universidad Politécnica de Cartagena, 30203 Cartagena (Murcia), Spain. Email: joaquin.zueco.upct.es

**O. Anwar Bég ^**

Professor of Aerodynamics Education, Aerosciences Program, BAE Systems, Salwa Garden Village, Villa G09D, PO Box 1732, Riyadh 11441, Kingdom of Saudi Arabia.

**H. S. Takhar**

Visiting Professor of Thermofluid Dynamics, Engineering Department, Manchester Metropolitan University, Oxford Rd., Manchester, M15GD, UK. Email: h.s.takhar@mmu.ac.uk

**V. R. Prasad**

Heat Transfer Research, 3-55 T.C., Bangalore Road, Madanapalle, 517325 (A.P.), India.

---

## Abstract

A two-dimensional mathematical model is presented for the laminar heat and mass transfer of an electrically-conducting, heat generating/absorbing fluid past a perforated horizontal surface in the presence viscous and Joule (Ohmic) heating. The Talbot-Cheng-Scheffer-Willis formulation (1980) is used to introduce a thermophoretic coefficient into the concentration boundary layer equation. The governing partial differential equations are non-dimensionalized and transformed into a system of nonlinear ordinary differential similarity equations, in a single independent variable,  $\eta$ . The resulting coupled, nonlinear equations are solved under appropriate transformed boundary conditions using the Network Simulation Method. Computations are performed for a wide range of the governing flow parameters, viz Prandtl number, thermophoretic coefficient (a function of Knudsen number), Eckert number (viscous heating effect), thermal conductivity parameter, heat absorption/generation parameter, wall transpiration parameter, Hartmann number and Schmidt number. The numerical details are discussed with relevant applications. Excellent correlation is achieved with earlier studies due to White (1974) and Chamkha and Issa (2000). The present problem finds applications in optical fiber fabrication, aerosol filter precipitators, particle deposition on hydronautical blades, semiconductor wafer design, thermo-electronics and nuclear hazards.

Key words: Thermophoresis; magnetohydrodynamics, heat and mass transfer; Prandtl number; Knudsen number; Hartmann number; Eckert number; Schmidt number; network simulation model, heat sinks/sources.

\* Author to whom correspondence should be addressed.

^ Also Director, Engovation Engineering Sciences, Great Horton, Bradford, BD7 3NU, England, UK. Email: docoabeg@hotmail.com.

The authors (all of different institutes) have formed a robust interdisciplinary applied thermal engineering research program since early 2007. This has involved the theoretical and numerical simulation of many diverse, advanced thermofluid dynamics problems. We have developed numerous novel mathematical models focused on rotating hydromagnetic plasma flows, hypersonic stagnation flows, rotating geophysical flows, thermophoretic deposition flows, pulsating biofluids, magnetic squeeze film lubrication, porous media geothermics, stratified flows and also thermal radiation flows. Many of our collaborations have now been published in leading international mechanical engineering and aerospace engineering journals.

---

## 1. INTRODUCTION

Thermophoresis is the migration of aerosol and other particles in the direction of a decreasing temperature gradient. Such a phenomenon has received considerable attention in the engineering analysis community owing to major applications in optical fiber production, heat exchanger fouling, aerosol reactors etc. In optical fiber synthesis, thermophoresis has been identified as the principal mechanism of mass transfer as used in the technique of modified chemical vapour deposition (MCVD) [1]. In this procedure a gaseous mixture of reactive precursors is directed over a heated substrate where solid film deposits are located. In particular the mathematical modeling of the deposition of silicon thin films using MCVD methods has been accelerated by the quality control measures enforced by the micro-electronics industry. Such topics involve a variety of complex fluid dynamical processes including thermophoretic transport of particulate deposits, heterogenous/homogenous chemical reactions, homogenous particulate nucleation and coupled heat and energy transfer. Boundary layer theory has proven to be instrumental in simplifying the flow regimes to facilitate numerical solutions via CFD and also user-specified numerical codes. Thermophoresis is also a key mechanism of study in semi-conductor technology, especially controlled high-quality wafer production as well as in radioactive particle deposition in nuclear reactor safety simulations and MHD energy generation system operations. A number of analytical and experimental papers in thermophoretic heat and mass transfer have been communicated. Brock [2] provided an early analysis of aerosol thermophoretic dynamics. Batchelor and Shen [3] later analyzed the thermophoretic migration of particles in a gaseous flow. Goren [4] considered the thermophoretic deposition of particles in flat plate boundary layers. Talbot et al [5] presented a seminal study, considering boundary layer flow with thermophoretic effects, which has become a benchmark for subsequent studies (this model is extended in the present paper). The thermophoretic flow of larger diameter particles was investigated by Kanki et al [6]. Lin and Ahn [7] studied thermophoretic flows in semi-conductor materials. Shen [8] discussed thermophoresis in two-dimensional and axisymmetric flow near cooled bodies. Sasse et al [9] considered laminar thermophoretic flows in various flat surface and concentric geometries. Yalamov and D'yakonov [10] presented more recently an analysis of the slow, steady-state thermophoresis of aggregates of aerosol particles. In this study the thermophoretic transfer was simulated via thermal slip of the surrounding gas along the particle surfaces. The temperature field near to the aggregate was used to compute, with the

method of successive approximations, the velocity of the thermophoretic aggregate particle motion. Konstandopoulos [11] discussed an Eulerian transport model for thermophoretic aerosol transport incorporating diffusion and also sub-critical inertial drift effects. Later Konstandopoulos and Rosner [12] showed numerically, using the FLUENT CFD software, that particles in thermophoretic transport can be simulated as a “fluid phase” governed by an asymptotic velocity field. Konstandopoulos and Rosner [13] also performed experiments to verify their numerical studies for thermophoretic transport to curved streamline boundaries. More recently Tsai [14] described the effects of lateral mass flux (suction) and thermophoresis in laminar boundary layers. An excellent study of free and forced convective boundary layer heat transfer with thermophoretic effects was reported by Chang et al [15]. Ahmadi and He [16] also studied thermophoretic effects but in both laminar and turbulent flows. Greenfield and Quarini [17] investigated computationally the thermophoresis effects on turbulent pipe flows. They compared numerical solutions with the STORM test data using a particle-tracking methodology to simulate the forces experienced by small particles in the opposite direction to the temperature gradient. More recently Chamkha and Pop [18] studied numerically the thermophoretic effects on double diffusive boundary layers in porous media using a Blottner difference technique. These studies were restricted to electrically non-conducting fluids. However in various industrial heat transfer processes, for example MHD energy systems, both thermophoresis and hydromagnetic flows take place simultaneously. Many numerical studies investigating magnetohydrodynamic heat (and mass) transfer have been reported with buoyancy, heat source/sink and also Joule heating effects. Takhar and Beg [19] studied the hydromagnetic free convection boundary layers in non-Darcian regimes using the Keller Box method. Other hydromagnetic convection flow studies include [20] which studied non-Newtonian wedge flow hydromagnetics, [21] which examined dissipative hydromagnetic boundary layers with wall suction/injection in porous media and [22] which studied the two-dimensional hydromagnetic flow with dissipation of a ferrofluid in a triangular enclosure. Beg et al [23] used a perturbation approach to study the transient oscillatory magnetohydrodynamic convection past a flat plate adjacent to a porous medium with heat generation effects. Zueco [24] studied computationally the transient natural convection hydromagnetics with viscous heating. Bég et al [25] studied numerically the magnetohydrodynamic flow of a gas from a spinning sphere with strong buoyancy using a finite difference method. Bég et al [26] have more recently used a finite element method to study the pulsating

dynamics of a hydromagnetic flow through a two-dimensional channel with mass transfer. Very recently Naroua et al [27] have also employed the finite element method to study the influence of electrodynamic Hall current and ionslip effects in strong magnetic cross fields on unsteady magneto-gas dynamic heat transfer from a spinning plate. These hydromagnetic studies have ignored thermophoretic effects. However Chamkha and Issa [28] presented a computational analysis of heat generation/absorption and thermophoresis on hydromagnetic flow with heat and mass transfer over a flat surface. In the present study we shall investigate numerically the steady two-dimensional heat and mass transfer in thermophoretic hydromagnetic flow over a flat plate with viscous heating, Joule heating, wall transpiration i.e. suction/injection, and heat source/sink effects. A network numerical simulation tool is employed which is described in detail later. Such a study has thusfar not appeared in the computational thermofluid dynamics literature, despite important applications in MHD energy systems, naval propulsion, magnetic materials processing etc.

## 2. MATHEMATICAL MODEL

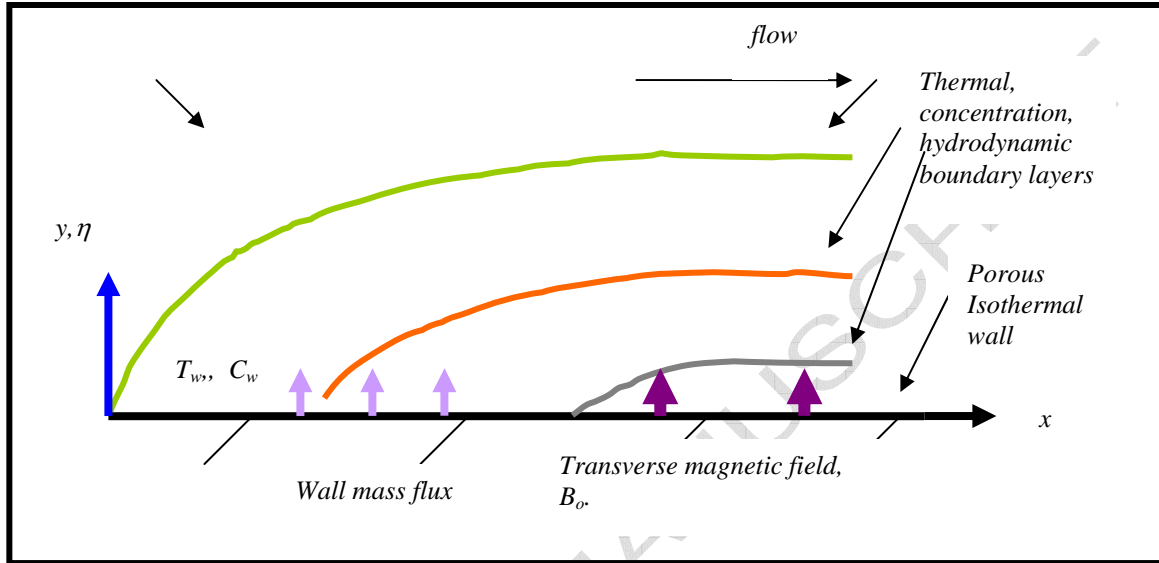
Consider the steady, dissipative laminar two-dimensional Newtonian heat and mass transfer over a flat surface with surface temperature  $T_w$ , surface concentration  $C_w$ , both constant and thermal conductivity,  $k_f$ , which obeys a linear temperature law according to  $k_f = k_o [1 + \alpha(T - T_\infty)] = k_o(1 + \beta\theta)$  where  $k_o$  denotes thermal conductivity in the free stream of the flow,  $\alpha$  is a thermophysical constant dependent on the fluid ( $\alpha < 0$  for lubrication oils, hydromagnetic working fluids and  $\alpha > 0$  for air or water) and  $\beta = \alpha(T_w - T_\infty)$  is the thermal conductivity variation parameter. A transverse magnetic field,  $\mathbf{B}$  acts perpendicular to the plate. Thermophoresis is present and the physical regime to be studied is illustrated below in figure 1. Magnetic Reynolds is assumed to be small enough to ignore induced magnetic field effects. The x direction is parallel to the plate and the y direction normal to this. Under the boundary-layer assumptions, the conservation equations for the flow regime can be shown to take the following form:

### **Conservation of Mass:**

$$\frac{\partial u}{\partial x} + \frac{\partial v}{\partial y} = 0 \quad (1)$$

**Conservation of Momentum :**

$$u \frac{\partial u}{\partial x} + v \frac{\partial u}{\partial y} = \nu \frac{\partial^2 u}{\partial y^2} - \frac{\sigma B^2(x)}{\rho} [u - u_\infty] \quad (2)$$

**Figure 1: Physical Model and Coordinate System****Conservation of Energy (Heat):**

$$u \frac{\partial T}{\partial x} + v \frac{\partial T}{\partial y} = \frac{1}{\rho c_p} \frac{\partial}{\partial y} \left[ k_f \frac{\partial T}{\partial y} \right] + \frac{\mu}{\rho c_p} \left[ \frac{\partial u}{\partial y} \right]^2 + \frac{\sigma B^2}{\rho c_p} [u - u_\infty]^2 + \frac{Q_o}{\rho c_p} [T - T_\infty] \quad (3)$$

**Conservation of Species (Concentration):**

$$u \frac{\partial C}{\partial x} + v \frac{\partial C}{\partial y} = D \frac{\partial^2 C}{\partial y^2} - \frac{\partial}{\partial y} (V_T C) \quad (4)$$

where  $u$  and  $v$  denote  $x$  and  $y$ -direction velocities,  $\nu$  is the kinematic fluid viscosity,  $\sigma$  is electrical conductivity,  $T$  is fluid temperature,  $C$  is species concentration (of particles),  $u_\infty$  and  $T_\infty$  are the free stream velocity and temperature,  $\rho$  is density,  $c_p$  is specific heat capacity of the fluid at constant pressure,  $D$  is the Fickian mass diffusion coefficient,  $V_T$

denotes thermophoretic velocity,  $B$  is the magnetic field strength,  $Q_0$  is heat source/sink parameter,  $\mu$  is dynamic viscosity of the fluid,  $k_f$  is the thermal conductivity of the fluid. The corresponding boundary conditions at the surface and far from the plate are:

$$u(x,0)=0; v(x,0)=-V_o(x); T(x,0)=T_w; C(x,0)=C_w \quad (5)$$

$$u(x,\infty)=u_\infty; T(x,\infty)=T_\infty; C(x,\infty)=C_\infty \text{ as } y \rightarrow \infty. \quad (6)$$

where  $V_o$  is the transpiration velocity at the wall. For *mass injection* into the boundary layer (blowing),  $V_o < 0$ ; for *mass removal* from the boundary layer (suction)  $V_o > 0$ .  $T_w$  is the wall temperature,  $C_w$  is the wall species concentration and  $C_\infty$  denotes particle concentration in the free stream i.e. outside the boundary layer. Following Talbot et al [5] we define the thermophoretic velocity as follows:

$$V_T = -k v \frac{\nabla T}{T} = -k v \frac{1}{T} \frac{\partial T}{\partial y} \quad (7)$$

where  $k v$  denotes the thermophoretic diffusivity and  $k$  is the *thermophoretic coefficient* defined, empirically, by Talbot et al [5] as:

$$k = \frac{2C_s \left[ \frac{k_f}{\lambda_p} + C_t Kn \right] C}{[1 + 3C_m Kn] \left[ 1 + \frac{2k_f}{\lambda_p} + 2C_t Kn \right]} \quad (8)$$

where  $k_f$  is the thermal conductivity of the fluid,  $\lambda_p$  is the thermal conductivity of the diffused particles,  $Kn$  is the Knudsen number and  $C_s$ ,  $C_t$  and  $C_m$  are empirical constants.  $Kn$  is a parameter generally used in rarefied aerodynamics and is defined by:

$$Kn = \bar{i} L_c \quad (9)$$

where  $\bar{i}$  is the mean free path of the particles and  $L_c$  denotes the characteristic length of the flow field. Following Shen [8], values of  $k$  are based on experimental values of  $C_s$ ,  $C_t$  and  $C_m$  and also  $Kn$  can be specified in thermophoretic simulations. For particle sizes less than 1 micron in diameter, it can be assumed to within a reasonable degree of

accuracy that  $k$  has values between 0.2 and 1.2. We shall adopt a value of 0.5 in our study. The equations (1) to (4) are strongly coupled, parabolic and nonlinear partial differential equations. An analytical solution cannot be obtained and therefore we seek numerical solutions. Numerical computations are greatly facilitated by non-dimensionalization of the equations. Proceeding with the analysis, we introduce the following similarity transformations and dimensionless variables which will convert the partial differential equations from two independent variables  $(x,y)$  to a system of coupled, non-linear ordinary differential equations in a single variable  $(\eta)$  i.e. coordinate normal to the plate. Following Chamkha and Issa [28] we define :

$$\eta = y \left( \frac{u_\infty}{2\nu x} \right)^{1/2} \quad (10)$$

$$\psi = (2\nu u_\infty x)^{1/2} \cdot f(\eta) \quad (11)$$

$$\theta = \frac{T - T_\infty}{T_w - T_\infty} \quad (12)$$

$$\Phi = \frac{C}{C_\infty} \quad (13)$$

$$u = \frac{\partial \psi}{\partial y} \quad (14)$$

$$v = - \frac{\partial \psi}{\partial x} \quad (15)$$

$$\text{Pr} = \frac{\mu c_p}{k_o} \quad (16)$$

$$f_o = 2V_o \left[ \frac{x}{2\nu u_\infty} \right]^{1/2} \quad (17)$$

$$Ha = \left[ \frac{2\sigma B^2}{\rho u_\infty} \right]^{1/2} \quad (18)$$

$$\Delta = \frac{2Q_o}{\rho c_p u_\infty} \quad (19)$$

$$Ec = \frac{u_\infty}{c_p [T_w - T_\infty]} \quad (20)$$

$$Sc = \frac{\nu}{D} \quad (21)$$

$$\tau = -k \left[ \frac{T_w - T_\infty}{T} \right] \quad (22)$$

where  $\psi$  is the stream function,  $\theta$  is non-dimensional temperature function,  $\Phi$  is non-dimensional concentration,  $Pr$  is Prandtl number,  $Sc$  is Schmidt number,  $\beta$  is non-dimensional thermal conductivity parameter,  $f_0$  is the dimensionless wall transpiration velocity (wall mass transfer coefficient),  $Ec$  is Eckert number,  $Ha$  is Hartmann number,  $\Delta$  is non-dimensional heat source/sink coefficient and  $\tau$  is dimensionless thermophoretic parameter. The mass conservation equation (1) is satisfied by the Cauchy-Riemann equations (14) and (15). A such "local similarity" is therefore employed. The equations of motion are thereby reduced from (2), (3) and (4) to the following dimensionless similarity form:

### **Momentum**

$$\frac{d^3 f}{d\eta^3} + f \frac{d^2 f}{d\eta^2} - Ha^2 \left[ \frac{df}{d\eta} - 1 \right] = 0 \quad (23)$$

### **Energy (Heat):**

$$\frac{d^2 \theta}{d\eta^2} [1 + \beta \theta] + \beta \left[ \frac{d\theta}{d\eta} \right]^2 + Pr f \frac{d\theta}{d\eta} + Ec Pr \left[ \frac{d^2 f}{d\eta^2} \right]^2 + Ec Ha^2 Pr \left[ \frac{df}{d\eta} - 1 \right]^2 + \Delta Pr \theta = 0 \quad (24)$$

### **Concentration:**

$$\frac{d^2 \Phi}{d\eta^2} + Sc \left[ \left( f - \tau \frac{d\theta}{d\eta} \right) \frac{d\Phi}{d\eta} - \tau \frac{d^2 \theta}{d\eta^2} \Phi \right] = 0 \quad (25)$$

The boundary conditions are also transformed to:

$$\text{At } \eta=0: \frac{df(0)}{d\eta} = 0; f(0) = f_0; \theta(0) = 1; \Phi(0) = 0 \quad (26)$$

$$\text{As } \eta \rightarrow \infty: \frac{df(\infty)}{d\eta} = 1; \theta(\infty) = 0; \Phi(\infty) = 1 \quad (27)$$

The model has been approximated for  $x=1$ , and as such this eliminates the need to solve for  $x$ . This makes the suction a constant and also eliminates the need to include  $x$  in equation (23). The system to be solved therefore is *seventh order* with *seven corresponding boundary conditions*. In (26)  $f_0$  may be positive for suction and negative for blowing. In (25) the thermophoretic parameter  $\tau$  assumes values of 0.01, 0.05 and 0.1 corresponding to the respective cases where  $-k(T_w - T_\infty)$  has values of 3, 15 and 30 Kelvins for a reference temperature of  $T = 293$  Kelvins (20 Celsius). We seek a full numerical solution to the transformed equations rather than analytical solutions. We shall herein dwell more on the physics of the flow regime. The general model defined by (23) to (25) with conditions (26) and (27) reduces to electrically non-conducting flow for  $Ha = 0$ , non-dissipative flow for  $Ec = 0$  and boundary layer flow past a solid wall for  $f_0 = 0$ .

### 3. NUMERICAL SOLUTION BY NETWORK SIMULATION METHOD

To solve the set of non-linear differential equation (23-25) subject to boundary condition (26, 27) the Network Simulation Method (NSM) has been applied. This method has been used successfully in a diverse variety of thermofluid problems. For example, Zueco et al [29] studied the unsteady thermal radiation in an enclosure using NSM. Other studies include [30], [31], [32]. The starting point is the set of ordinary differential equations, one for each control volume, obtained either by spatial discretization of the equations. Time remains as a continuous variable in the discretized equations so that no time interval needs to be formed for the numerical solution by the programmer. Based on these equations, a network circuit is designed, whose equations are formally equivalent to the discretized ones. The variables,  $f$ ,  $\theta$  and  $\Phi$  are equivalent to the variable voltage, and the derivatives of them are equivalent to the electric current. A sufficient number of networks are connected in series to form the whole medium and boundary conditions are added by means of special electrical devices. The whole network must be converted into an adequate program that can be solved by a computer code. Generally, few programming rules are necessary since the number of the electrical devices that make

up the network is very small. The cases studied here were solved by the software code Pspice [33] using a PC. To solve the set of non-linear differential equation (23-25) subject to boundary condition (26-27) the NSM has been applied. The equations (23-25) may be further written as,

$$\frac{df}{d\eta} = h \quad (28)$$

$$\frac{d^2h}{d\eta^2} + f \frac{dh}{d\eta} - Ha^2(h-1) = 0 \quad (29)$$

$$\frac{1}{Pr} \frac{d^2\theta}{d\eta^2} (1 + \beta\theta) + \frac{\beta}{Pr} \frac{d\theta}{d\eta} + f \frac{d\theta}{d\eta} + Ec \left[ \frac{dh}{d\eta} \right]^2 + EcHa^2(h-1)^2 + \Delta\theta = 0 \quad (30)$$

$$\frac{d^2\Phi}{d\eta^2} + Sc \left[ \left( f - \tau \frac{d\theta}{d\eta} \right) \frac{d\Phi}{d\eta} - \tau \frac{d^2\theta}{d\eta^2} \Phi \right] = 0 \quad (31)$$

The following currents are defined:

$$j_h \equiv \frac{dh}{d\eta} \quad (32)$$

$$j_\theta \equiv \frac{d\theta}{d\eta} \quad (33)$$

$$j_\Phi \equiv \frac{d\Phi}{d\eta} \quad (34)$$

With these definitions of the currents, the dimensionless equations of momentum, energy and concentration are re-written.

$$\frac{dj_h}{d\eta} + f \frac{dh}{d\eta} - Ha^2(h-1)^2 = 0 \quad (35)$$

$$\frac{dj_\theta}{d\eta}(1 + \beta\theta) + \beta \frac{d\theta}{d\eta} + \text{Pr}\left[f \frac{d\theta}{d\eta} + \text{Ec}\left(\frac{dh}{d\eta}\right)^2 + \text{EcHa}^2(h-1)^2 + \Delta\theta\right] = 0 \quad (36)$$

$$\frac{dj_\Phi}{d\eta} + \text{Sc}\left[\left(f - \tau \frac{d\theta}{d\eta}\right) \frac{d\Phi}{d\eta} - \tau \frac{dj_\theta}{d\eta} \Phi\right] = 0 \quad (37)$$

These are partial differential equations with two variables in each equation, With a spatial discretization of the dimensionless equations in N cells of length  $\Delta\eta = \eta_{\max}/N$ , with  $N=200$ ,  $\eta_{\max}=10$  (obtained after of to do probes numerical). These partial differential equation can be transformed into a system of *connected* differential equations by means of a second-order central difference scheme. It is considered a thickness of the elemental cell of  $\Delta\eta$  (not  $2\Delta\eta$ ), and calling “ $i-\Delta\eta$ ” and “ $i+\Delta\eta$ ” the extremes of the cell and “ $i$ ” the centre of the cell.

$$(\partial f / \partial \eta)_i \approx (f_{i+\Delta\eta} - f_{i-\Delta\eta}) / \Delta\eta \quad (38)$$

$$(\partial^2 h / \partial \eta^2)_i \approx [(h_{i-\Delta\eta} - h_i) / (\Delta\eta^2/2) - (h_i - h_{i+\Delta\eta}) / (\Delta\eta^2/2)] = (j_{hi-\Delta} - j_{hi+\Delta}) / \Delta\eta \quad (39)$$

$$(\partial^2 \theta / \partial \eta^2)_i \approx [(\theta_{i-\Delta\eta} - \theta_i) / (\Delta\eta^2/2) - (\theta_i - \theta_{i+\Delta\eta}) / (\Delta\eta^2/2)] = (j_{\theta i-\Delta} - j_{\theta i+\Delta}) / \Delta\eta \quad (40)$$

$$(\partial^2 \Phi / \partial \eta^2)_i \approx [(\Phi_{i-\Delta\eta} - \Phi_i) / (\Delta\eta^2/2) - (\Phi_i - \Phi_{i+\Delta\eta}) / (\Delta\eta^2/2)] = (j_{\Phi i-\Delta} - j_{\Phi i+\Delta}) / \Delta\eta \quad (41)$$

Therefore, the *finite-difference differential equations* are,

$$f_i = h_i \Delta\eta + f_{i-\Delta} \quad (42)$$

$$j_{hi-\Delta} - j_{hi+\Delta} + f_i (h_{i+\Delta} - h_{i-\Delta}) - \text{Ha}^2 (h_i - 1) = 0 \quad (43)$$

$$j_{\theta_{i-\Delta}} - j_{\theta_{i+\Delta}} + \frac{\beta}{(1 + \beta\theta_i)}(\theta_{i+\Delta} - \theta_{i-\Delta}) + \frac{\text{Pr}}{(1 + \beta\theta_i)}[f_i(\theta_{i+\Delta} - \theta_{i-\Delta}) + \text{Ec} \frac{(h_{i+\Delta} - h_{i-\Delta})^2}{\Delta\eta}] + \Delta\eta\text{EcHa}^2(h_i - 1)^2 + \Delta\eta\Delta\theta_i = 0 \quad (44)$$

$$j_{\Phi_{i-\Delta}} - j_{\Phi_{i+\Delta}} + \text{Sc}[(f_i - \tau(\theta_{i+\Delta} - \theta_{i-\Delta})/\Delta\eta)(\Phi_{i+\Delta} - \Phi_{i-\Delta}) - \tau(j_{\theta_{i-\Delta}} - j_{\theta_{i+\Delta}})\Phi_i] = 0 \quad (45)$$

where the term  $(j_{\theta_{i-\Delta}} - j_{\theta_{i+\Delta}})$  of the Eq. 45 is obtained of the Eq. 44.

Eqs. (43-45) can be taken as fulfilling Kirchhoff's current law (where all the terms can be treated as currents), while the variables  $f$ ,  $h$ ,  $\theta$  and  $\Phi$  satisfy Kirchhoff's voltage law since they are continuous and single-valued. Consequently, it is possible to analyse the thermophoretic hydromagnetic problem by an electrical network. Hence, Eqs. (38-40) define two resistors of a same value  $\Delta\eta/2$  by each elemental network model (there is three, one for each equation). A resistor is connecting between the left extreme ( $i-\Delta\eta$ ) and the centre of the cell ( $i$ ), and the other resistor is connecting between the centre and the right extreme ( $i+\Delta\eta$ ) of the elemental cell. The others terms of the equations are implemented by means of current sources controlled by voltage connecting to the centre of the cell ( $i$ ). Connecting  $N$  basic circuits in series gives the network representing the one-dimensional medium in which the velocity, temperature and concentration are coupled. The next step is to include the initial and boundary conditions in the network model. Eqs. (26, 27) at the limits  $\eta = 0$  and  $\eta = \infty$ , which is reflected in the network model by connecting a voltage source of value the unity for the temperature and of zero value for the velocity and concentration between the free end of the first cell and ground, while the opposite is considered between the free end of the last cell and ground.

There are eight governing parameters,  $\text{Ha}$ ,  $\text{Ec}$ ,  $\Delta$ ,  $\text{Pr}$ ,  $\text{Sc}$ ,  $\beta$ ,  $f_0$  and  $\tau$ . We have obtained comprehensive solutions for the influence of these parameters on *dimensionless velocity* ( $df/d\eta$ ), *dimensionless temperature* ( $\theta$ ) and *dimensionless concentration of particles* ( $\Phi$ ). Comparison has been made (not plotted) with the studies of White [34] and Chamkha and Issa [28] which *did not consider thermal conductivity variation, ignored viscous and Joule heating and considered a solid wall*.

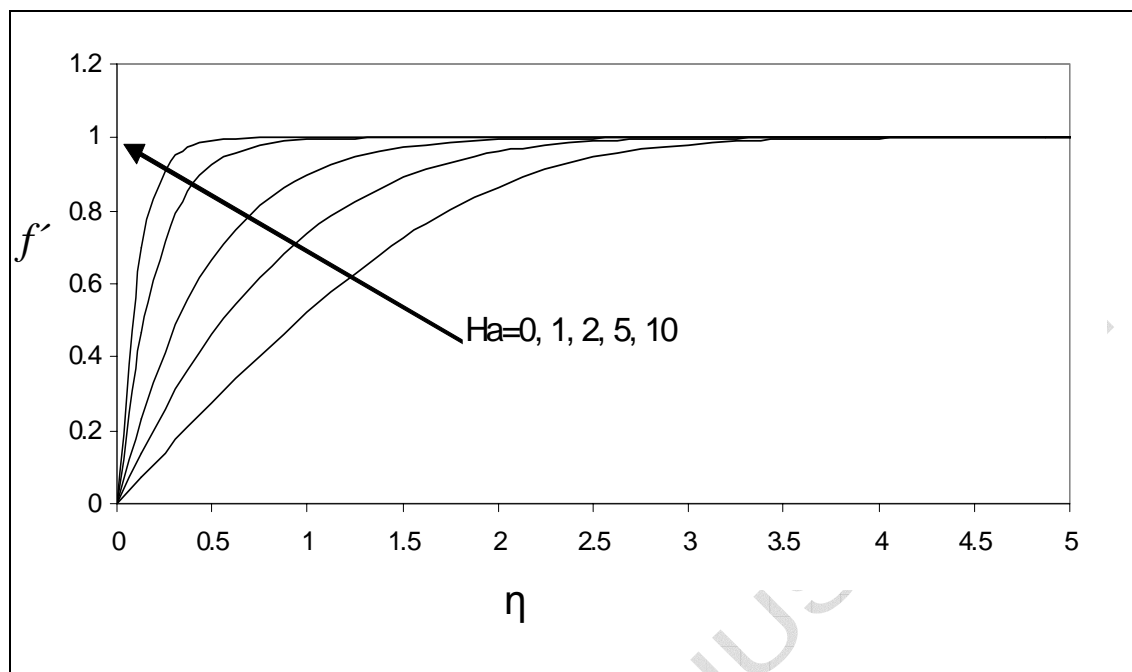


**Figure 2: Dimensionless velocity ( $df/d\eta$ ) versus  $\eta$  for  $Ha = 0, 1, 2, 5, 10$  with  $Ec = 0.1, \Delta = 0.1, Pr = 0.7, Sc = 0.6, \beta = 0.5, f_0 = 0.1, \tau = 0.5$ .**

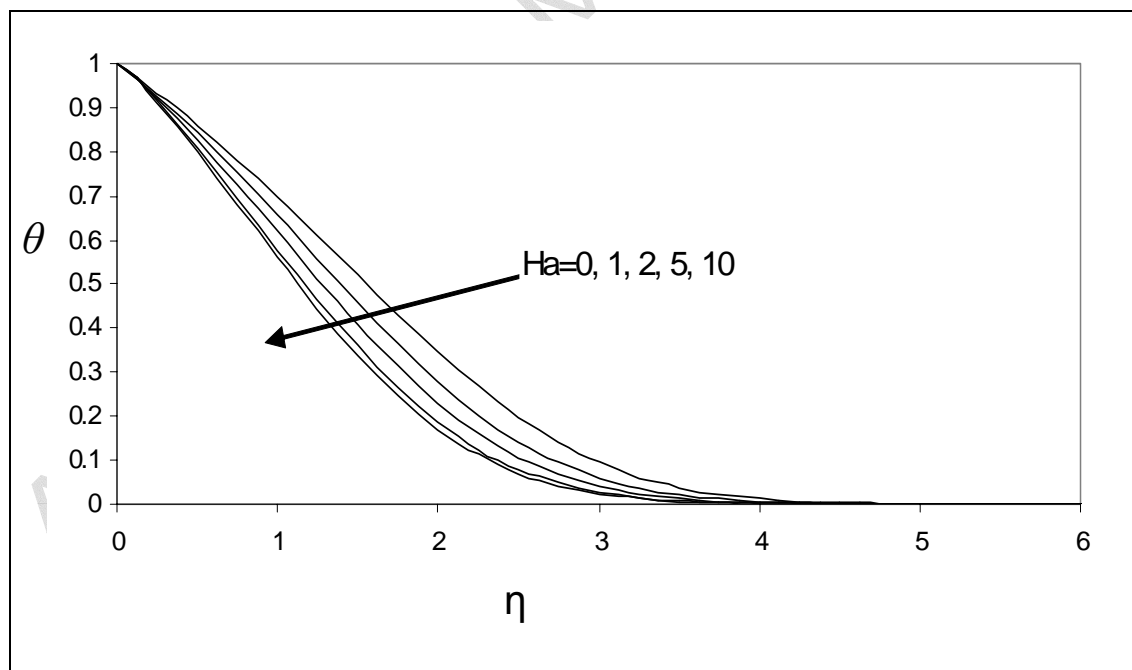


**Figure 3: Dimensionless temperature ( $\theta$ ) versus  $\eta$  for  $Ha = 0, 1, 2, 5, 10$  with  $Ec = 0.1, \Delta = 0.1, Pr = 0.7, Sc = 0.6, \beta = 0.5, f_0 = 0.1, \tau = 0.5$ .**

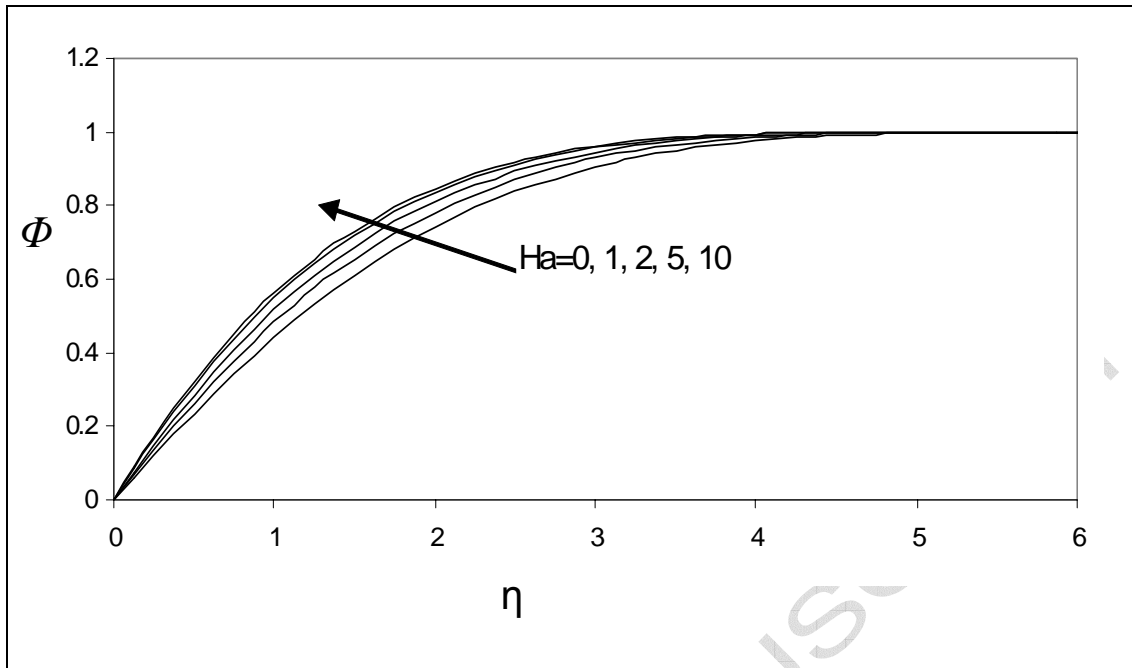


**Figure 4: Dimensionless concentration ( $\Phi$ ) versus  $\eta$  for  $Ha = 0, 1, 2, 5, 10$  with  $Ec = 0.1, \Delta = 0.1, Pr = 0.7, Sc = 0.6, \beta = 0.5, f_0 = 0.1, \tau = 0.5$ .**

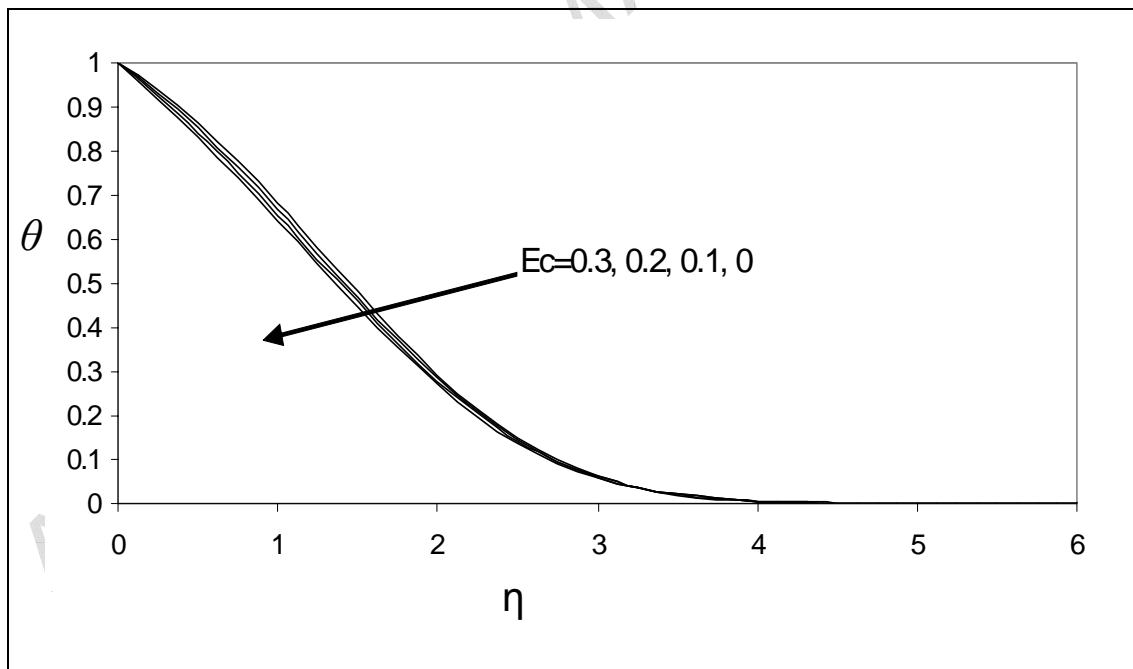


**Figure 5: Dimensionless temperature ( $\theta$ ) versus  $\eta$  for  $Ec = 0, 0.1, 0.2, 0.3$ , with  $Ha = 1, \Delta = 0.1, Pr = 0.7, Sc = 0.6, \beta = 0.5, f_0 = 0.1, \tau = 0.5$ .**

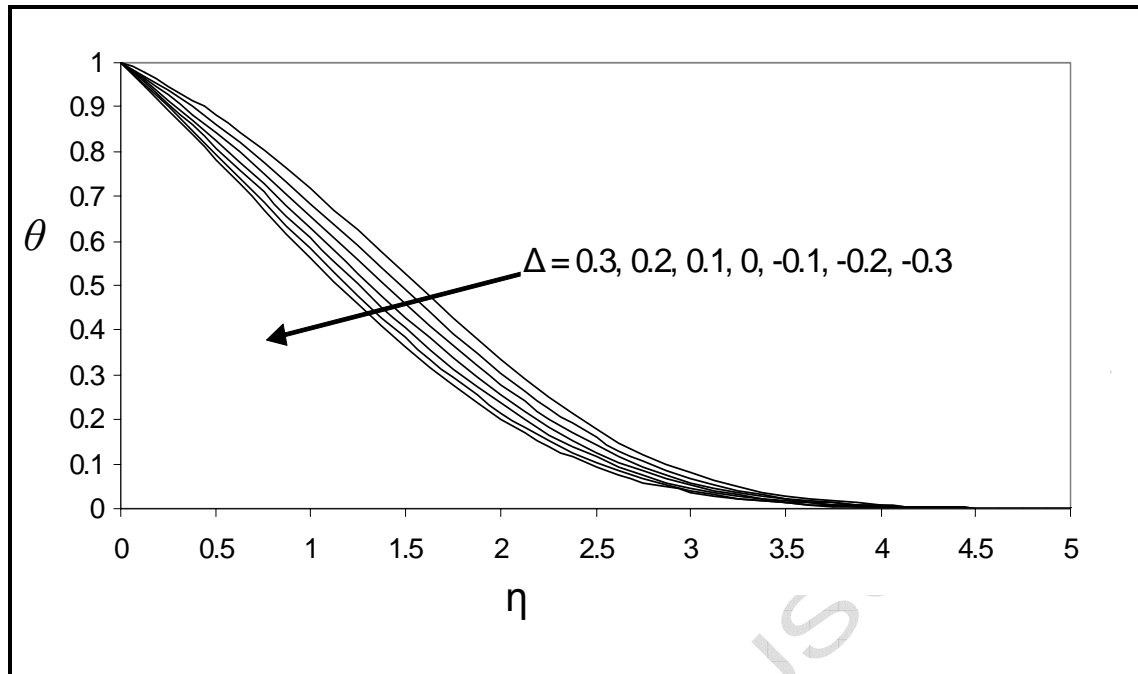


**Figure 6: Dimensionless temperature ( $\theta$ ) versus  $\eta$  for  $\Delta = -0.7, -0.2, 0, 0.2, 0.7$  with  $Ha = 1, Ec = 0.1, Pr = 0.7, Sc = 0.6, \beta = 0.5, f_0 = 0.1, \tau = 0.5$ .**

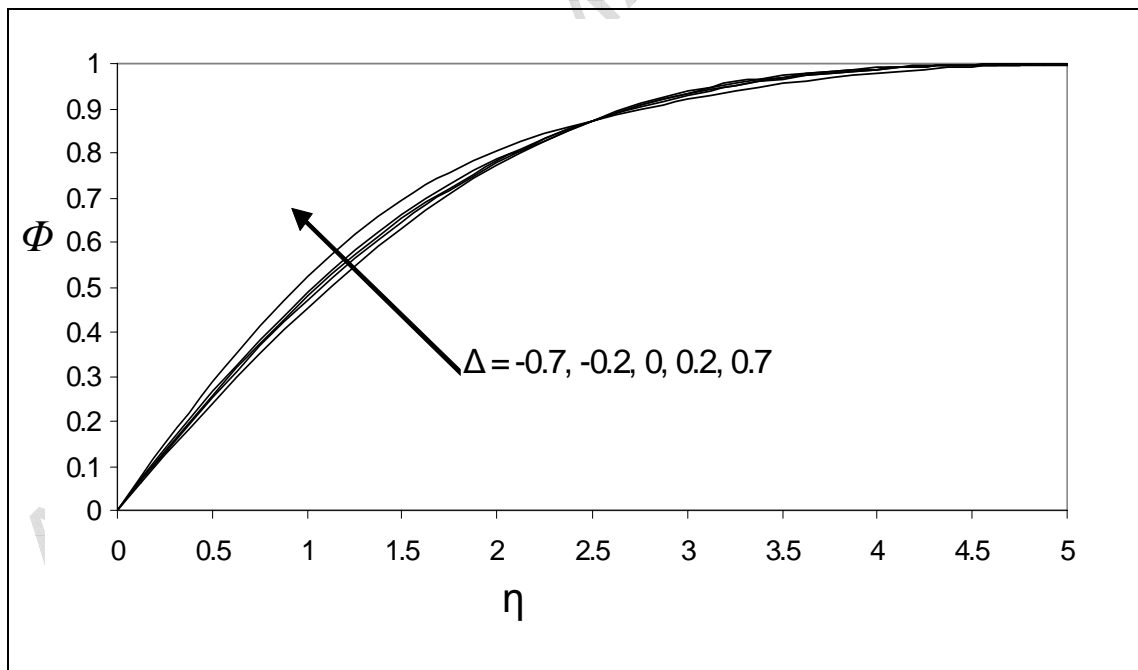


**Figure 7: Dimensionless concentration ( $\Phi$ ) versus  $\eta$  for  $\Delta = -0.7, -0.2, 0, 0.2, 0.7$  with  $Ha = 1, Ec = 0.1, Pr = 0.7, Sc = 0.6, \beta = 0.5, f_0 = 0.1, \tau = 0.5$ .**

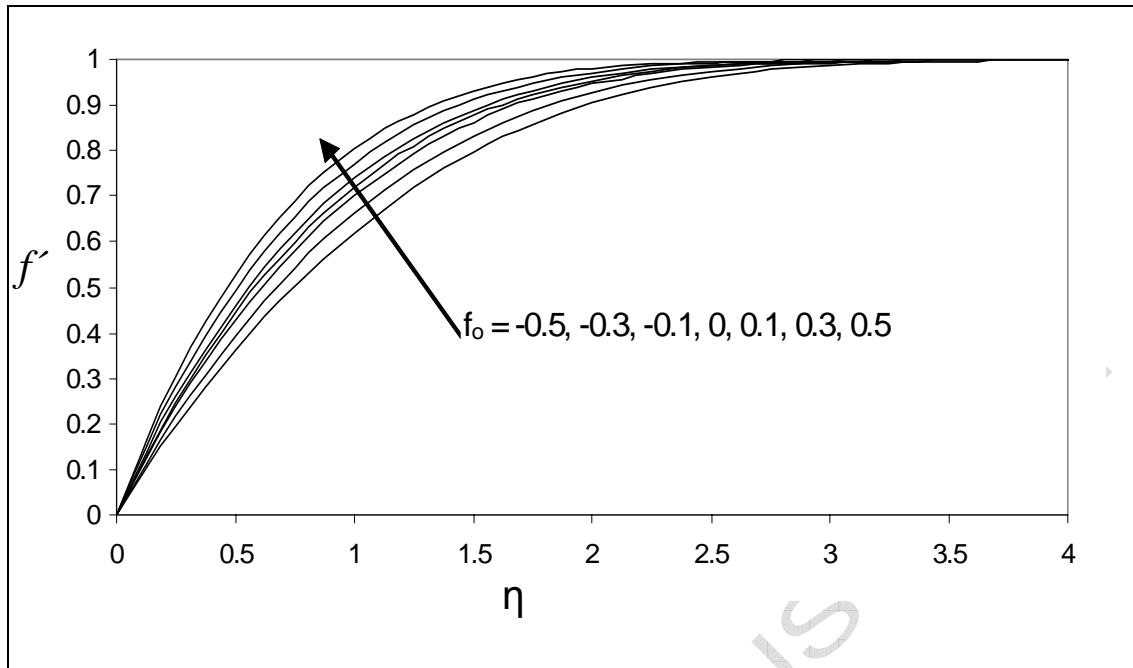


**Figure 8: Dimensionless velocity ( $df/d\eta$ ) versus  $\eta$  for  $f_0 = -0.5, -0.3, -0.1$  (injection), **0** (solid wall), **0.1, 0.3, 0.5** (wall suction) with  $Ha = 1$ ,  $Ec = 0.1$ ,  $\Delta = 0.1$ ,  $Pr = 0.7$ ,  $Sc = 0.6$ ,  $\beta = 0.5$ ,  $\tau = 0.5$ .**

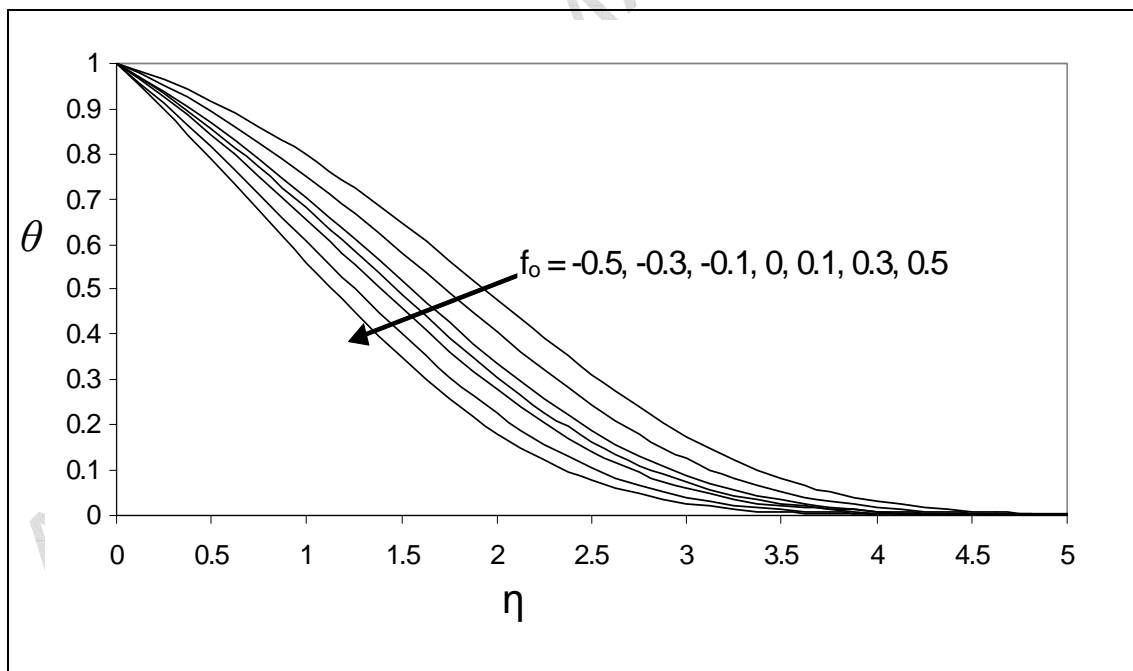


**Figure 9: Dimensionless temperature ( $\theta$ ) versus  $\eta$  for  $f_0 = -0.5, -0.3, -0.1$  (injection), **0** (solid wall), **0.1, 0.3, 0.5** (wall suction) with  $Ha = 1$ ,  $Ec = 0.1$ ,  $\Delta = 0.1$ ,  $Pr = 0.7$ ,  $Sc = 0.6$ ,  $\beta = 0.5$ ,  $\tau = 0.5$ .**

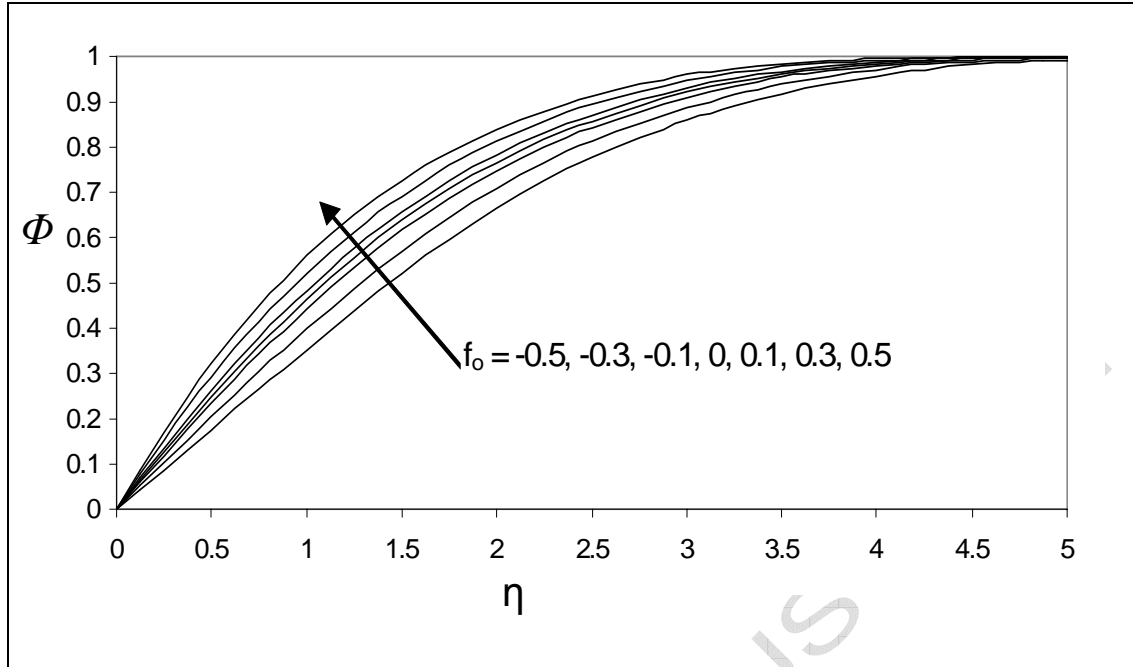


**Figure 10: Dimensionless concentration ( $\Phi$ ) versus  $\eta$  for  $f_0 = -0.5, -0.3, -0.1$  (injection),  $0$  (solid wall),  $0.1, 0.3, 0.5$  (wall suction) with  $Ha = 1$ ,  $Ec = 0.1$ ,  $\Delta = 0.1$ ,  $Pr = 0.7$ ,  $Sc = 0.6$ ,  $\beta = 0.5$ ,  $\tau = 0.5$ .**

#### 4. RESULTS AND DISCUSSION

In the present computations we have set the following default values for the governing thermophysical parameters:  $Ha = 1$ ,  $Ec = 0.1$ ,  $\Delta = 0.1$ ,  $Pr = 0.7$ ,  $Sc = 0.6$ ,  $\beta = 0.5$ ,  $f_0 = 0.1$  and  $\tau = 0.5$ . As such the flow is weakly hydromagnetic, buoyancy-driven double-diffusive thermal convection of gas diffusing in air, with wall suction. In the momentum

equation,  $\frac{d^3 f}{d\eta^3} + f \frac{d^2 f}{d\eta^2} - Ha^2 \left[ \frac{df}{d\eta} - 1 \right] = 0$ , the hydromagnetic drag is found to aid

*velocity* development, rather than incur it. This deviates from classical Hartmann channel flow owing to the presence of a negative unity term in the magnetic term. This result has also been identified by Chamkha and Issa [34]. Since  $Ha^2$  is always positive, and  $df/d\eta \leq$

1 (due to boundary conditions), effectively the  $-Ha^2 \left[ \frac{df}{d\eta} - 1 \right]$  term in the momentum

equation, will assume a positive value for  $df/d\eta < 1$  (it will vanish when  $df/d\eta = 1$ ). As a result Hartmann number will have a positive effect on the fluid development i.e. generate acceleration. This effect is further demonstrated in **figure 2** where we observe a strong increase in dimensionless velocity, in particular near the wall as  $Ha$  is increased

from 0 (electrically non-conducting case) through 1, 2, 5 and 10. Maximum velocity therefore accompanies maximum Hartmann number. High  $Ha$  profiles are seen to ascend more rapidly over the near-wall regime,  $0 < \eta < 0.5$ ; all profiles however converge to a value of unity at  $\eta \sim 3.5$ . The reason magnetic parameter ( $Ha$ ) increases velocity ( $f'$ ) is because the magnetic field is moving with the free stream due to the term  $Ha^2 (f'-1)$  in equation (23) and this will increase velocities, not retard them (as in classical MHD boundary layer flow or Hartmann channel flow). The variation of dimensionless temperature,  $\theta$ , with  $\eta$  for various Hartmann numbers is shown in **figure 3**.  $Ha$  effects are experienced in the energy conservation equation (24) via the Joule heating (i.e. Ohmic) term,  $EcHa^2 Pr[\frac{df}{d\eta} - 1]^2$ . Clearly temperatures are seen to be reduced considerably with an increase in  $Ha$  from 0 through 1, 5 to 10. All profiles decay from a maximum temperature at the wall, to zero in the free stream. Joule heating is generated due to resistance of the fluid to the flow of current. Magnetic field does not alter the total energy in the boundary layer regime. The kinetic energy lost from the fluid flow due to magnetic field effects is manifested as Joule (Ohmic) heating. We therefore expect in classical magnetofluid boundary layer flow an increase in temperatures with an increase in magnetic field effect i.e. Hartmann number. However the augmentation of the standard velocity  $df/d\eta$ , to  $[df/d\eta - 1]$  in the Joule heating term,  $EcHa^2 Pr[\frac{df}{d\eta} - 1]^2$ , serves to reverse this trend. Since magnetic field effectively accelerates the flow [i.e. in this flow scenario velocity is boosted by a rise in  $Ha$ , as depicted in figure 2], thermal energy will be replaced by kinetic energy and this will lower the fluid temperature away from the plate surface i.e. through the boundary layer, as  $Ha$  is increased. The trend of the results is therefore consistent with Chamkha and Issa [28]. **Figure 4** shows the distribution of dimensionless concentration through the boundary layer with increasing Hartmann number,  $Ha$ . In this figure we observe that concentration value,  $\Phi$ , is converse to velocity or temperature, minimized for the non-conducting case ( $Ha = 0$ ).  $\Phi$  values are increased with a rise in  $Ha$  i.e. mass diffusion is boosted with increasing magnetic field. All profiles increase monotonically from 0 at the wall to unity in the free stream, with profiles converging further from the wall, around  $\eta \sim 5$ .

The influence of Eckert number on dimensionless temperature and concentration functions is shown in **figure 5**. Eckert number, symbolized by  $Ec = \frac{u_\infty}{c_p [T_w - T_\infty]}$ , and

appearing firstly in (24) in the term,  $+ Ec \text{Pr} \left[ \frac{d^2 f}{d\eta^2} \right]^2$ , designates the *ratio of the kinetic*

*energy of the flow to the boundary layer enthalpy difference*. Although  $Ec$  is used in high altitude rocket aero-thermodynamics (where the prescribed temperature difference is of the same order of magnitude as the absolute temperature in the free stream), in the context of *low speed incompressible flows*, as described in the present paper, it signifies the difference between the total mechanical power input and the smaller amount of total power input which produces thermodynamically reversible effects i.e. elevations in kinetic and potential energy. This difference constitutes the energy dissipated as thermal energy by viscous effects i.e. work done by the viscous fluid in overcoming internal friction, hence the term *viscous heating*. Positive values of  $Ec$  correspond to plate cooling i.e. loss of heat from the plate to the fluid; negative values imply the reverse i.e. plate heating wherein heat is received by the plate from the fluid. In this article we concentrate on the former case.  $Ec$  also appears in the Joule (Ohmic) heating hydromagnetic term in equation (24), viz  $+ Ec Ha^2 \text{Pr} \left[ \frac{df}{d\eta} - 1 \right]^2$ . As such for non-zero

magnetic field, considered in figure 5 ( $Ha = 1$ ), Joule heating will also be present. We observe that a rise in  $Ec$  from 0 (no dissipation) through 0.1, 0.2 to 0.3 causes a noticeable increase in temperature,  $\theta$ , in particular in the near-wall region. All profiles decay asymptotically from a maximum wall temperature (unity) to zero in the free stream. Maximum fluid temperature in the boundary layer therefore is associated with the maximum  $Ec$  value, which is physically valid since greater thermal energy is generated in the fluid for larger  $Ec$  values. The influence of  $Ec$  on dimensionless concentration function (no plotted),  $\Phi$  as expected is negligible.

**Figures 6 and 7** to illustrate the influence of heat generation/absorption parameter,  $\Delta$ , on the dimensionless temperature and concentration fields through the boundary-layer. As expected a rise in positive value of  $\Delta$  from 0 to 0.1, 0.2 and 0.3 induces a clear increase in temperature function,  $\theta$ , throughout the flow domain normal to the plate. Physically heat generation in the fluid will add thermal energy to the flow and therefore for positive  $\Delta$  temperatures will rise. Such a *heat source phenomenon* is possible in

energy system devices or hot spots in industrial treatment systems. Conversely an increase in negative value of  $\Delta$  from -0.1 to -0.2 and -0.3 will remove thermal energy from the flow i.e. act as a heat sink causing temperatures to drop. This indeed is shown in **figure 6**. The case of no heat source/sink logically lies at the interface between the minimal values of positive and negative  $\Delta$ . The trend for all temperature plots, in consistency with the wall and free stream boundary conditions is a gradual decay from the plate (wall) to the edge of the boundary layer, where we observe all profiles converging to zero at approximately  $\eta = 4$ . These effects are very similar to non-magnetic studies, indicating that heat source/sink effects are not influenced by the presence of a transverse magnetic field. A similar but less dramatic trend is observed for the distribution of concentration,  $\Phi$  in the domain (**figure 7**). Again  $\Phi$  is increased with a positive rise in  $\Delta$  i.e. increasing heat generation, but lowered with an increase in negative  $\Delta$  from -0.2 to -0.7.

The effects of lateral wall mass flux (suction/injection) on dimensionless velocity, temperature and concentration are illustrated in **figures 8 to 10**. Velocity is seen to be increased with a rise in suction parameter ( $f_0 > 0$ ) but decreased with a rise in injection (blowing) at the wall ( $f_0 < 0$ ). Material removal from the boundary layer i.e. suction causes the fluid to accelerate normal to the wall resulting in a rise in values of  $f'$  i.e.  $df/d\eta$  as  $f_0$  rises from 0 (solid wall) to 0.1, 0.3 and 0.5. These results are very similar to the non-magnetic study by Tsai [37]. Conversely blowing i.e. negative wall mass flux induces a deceleration in the flow in the boundary layer causing a decrease in velocity. The lowest velocity computed thereby correspond to the maximum value of wall injection i.e.  $f_0 = -0.5$ , with the maximum velocity corresponding to the maximum value of wall suction i.e.  $f_0 = +0.5$ . The strong influence of wall flux on flow acceleration/deceleration indicates that even with thermophoresis present ( $\tau > 0$ ) a porous wall can be a powerful mechanism for controlling momentum of the boundary layer regime flow in actual applications e.g. optical fiber manufacture, particle deposition on turbine blades in naval propulsion etc. The profiles computed all ascend in **figure 8** from zero at the wall (no-slip) to a maximum of unity in the free stream. The effects of wall mass flux are of course maximized in the near-wall regime in particular in the vicinity of  $\eta = 1$ . **Figure 9** shows that wall suction causes a strong decrease in temperature function ( $\theta$ ) throughout the boundary-layer regime, while wall injection (blowing) induces an increase in temperatures. Effects of wall mass flux parameter,  $f_0$ , are maximized close to the wall, as

expected, around  $\eta = 2$ . **Figure 10** illustrates that as with the velocity field, wall suction induces a positive effect i.e. increase in dimensionless concentration function,  $\Phi$ , whereas wall injection decreases  $\Phi$ . As such then the presence of wall suction increases velocity and concentration boundary layer thicknesses but decreases the thermal boundary layer thickness. i.e. *thins out the thermal boundary layer*.

These results are of significance in actual operations in for example the magnetic field control of particle deposition in chemical vapour processing. Hsu and Grief [38] have identified that the attainment of high particle deposition efficiency and the accurate regulation of the deposition to minimize operational costs and maximize the quality of the final product requires theoretical analysis of thermophoretic boundary layer flows. High efficiency *and control* of deposition, the latter achievable via *magnetic field application*, directly influence the success of the chemical vapor deposition in working systems in industry. Understanding boundary layer thermophoretic deposition flows and also stagnation deposition flows is significant since these arise in various heat exchanger systems where flows are present on solid or porous walls [38]. Blums and Odenbach [39] have further highlighted the very important need to model accurately the boundary layer flows with thermophoresis *and magnetic fields*. The high thermophoretic mobility of nano-meter-scaled magnetite particles in magnetic fluids necessitates the correct modeling of such flows using thermal boundary layer magnetohydrodynamics with thermophoresis present. The results of such investigations can aid in identifying the best range of operations of deposition processes and can confirm the practical efficiency of using a magnetic field. This has been employed in for example in Blums et al [40] which discusses particle separation in *ferrocolloids*, a new group of fluids being employed in state-of-the-art deposition processes in heat exchanger and other applied thermal engineering operations. Zahmatkesh [41] has further emphasized the need for analyzing boundary layer phenomena with thermophoresis (and also Brownian diffusion) indicating that fundamental fluid dynamics models must be employed to simulate flows involving thermophoresis to provide a guide to industrial designers of deposition processes. Thermophoresis is important since designers of applied thermal systems must achieve a migration of particles away from hot surfaces where boundary layers arise. The net force acting in the opposite direction to the temperature gradient, i.e. towards the low temperature region is a direct consequence of the differential bombardment of gas molecules which originate from the relatively hot and cold regions in the vicinity of particles. The present numerical study has investigated this successfully and has

provided *important benchmark data for more advanced numerical simulations of interest to thermal designers*. Furthermore the present study provides a solid platform on which to elucidate the complex phenomena encountered in for example directional flows in tin-bismuth alloy deposition processes [42] in which better control of thermophoresis is attained with magnetic field imposition, as discussed at length by Bacri et al [42].

## 5. CONCLUSIONS

In this article a mathematical model has been presented for the hydromagnetic boundary layer flow past a porous flat surface with thermophoresis present and also heat source/sink effects and viscous and Joule heating. Using transformations a set of ordinary differential equations has been derived for the conservation of mass, momentum and species diffusion in the boundary layer regime. These nonlinear, coupled differential equations have been solved under physically valid boundary conditions using a robust numerical method known as Network Simulation. Our computations have confirmed the earlier solutions reported by Chamkha and Issa [28] and also the non-magnetic analysis reported in White [34]. Suction has been shown to increase fluid velocity and concentration but to lower temperatures. Magnetic field (i.e. Hartmann number) has been shown in the present flow scenario to in fact induce acceleration of the flow, rather than deceleration, but to reduce temperatures and increase concentration of particles in the boundary layer. A positive increase in Eckert number is shown to reduce temperatures in the flow, as experienced via both viscous dissipation and Joule (Ohmic) heating. Thermophoresis for the case of a cold wall (positive  $\tau$ ) is shown to initially increase concentration of particles in the boundary layer, but a short distance from the wall this trend is reversed. The computations have important implications in aerosol deposition dynamics, hydronautics of blades, and also optical fiber manufacture under magnetic field control.

## 6. REFERENCES

- [1] Kremer, D. M., Davis, R.W., Moore, E.F., Maslar, J.E., Burgess, D.R. and Ehrman, S.H., **J. Electrochemical Society**, 150, 2, G127-G139 (2003).
- [2] Brock, J.R., On the theory of thermal forces acting on aerosol particles, **J. Colloid. Sci.**, 17, 768-780 (1962).

- [3] Batchelor, G.K. and Shen, C., Thermophoretic deposition of particles in gas flowing over cold surfaces, **J. Colloid. Interf. Sci.**, 107, 1, 21-37 (1985).
- [4] Goren, S.L., The role of thermophoresis of laminar flow of a viscous and incompressible fluid, **J. Colloid. Interf. Sci.**, 61, 77 (1977).
- [5] Talbot, L., Cheng, R.K., Schefer, R.W. and Willis, D.R., Thermophoresis of particles in a heated boundary layer, **J. Fluid Mech.**, 101, 4, 737-758 (1980).
- [6] Kanki, T., Iuchi, S., Miyazaki, T. and Ueda, H., On thermophoresis of relatively large aerosol particles suspended near a plate, **J. Colloid. Interf. Sci.**, 107, 2, 418-425 (1985).
- [7] Lin, B.Y.H. and Ahn, K., Particle deposition on semiconductor wafers, **Aerosol Sci. Tech.**, 6, 215-224 (1987).
- [8] Shen, C. Thermophoretic deposition of particles onto cold surface of bodies in two-dimensional and axi-symmetric flows, **J. Colloid. Interf. Sci.**, 127, 104-115 (1988).
- [9] Sasse, A.G. B. M., Nazaroff, W.W. and Gadgil, A.J., Thermophoretic removal of particles from laminar flow between parallel plates and concentric tubes, **Am. Assoc. Aerosol. Res. Conf., San Francisco, California, 12-16 October** (1992).
- [10] Yalamov, Y. I. and D'yakonov, S.N., Thermophoresis of an aggregate of two large solid spheres in contact with each other along their center line: Part I- Thermal problem, **High Temperature J (Heat and Mass Transfer and Physical Gas Dynamics)**, 35, 1 (1997).
- [11] Konstandopoulos, A.G., Effect of particle inertia on aerosol transport and deposit growth dynamics, **PhD dissertation, Chemical Engineering, Yale University, New Haven, Connecticut, USA** (1991).
- [12] Konstandopoulos, A.G. and Rosner, D.E., Inertial effects on thermophoretic transport of small particles to walls with streamwise curvature, Part I: Theory, **Int. J. Heat Mass Transfer**, 38, 12, 2305-2315 (1995).
- [13] Konstandopoulos, A.G. and Rosner, D.E., Inertial effects on thermophoretic transport of small particles to walls with streamwise curvature, Part II: Experiment, **Int. J. Heat Mass Transfer**, 38, 12, 2317-2327 (1995).
- [14] O. A. Bég , Thermophoretic thermal boundary layer flows: a review, **Technical Report**, Leeds, December (2005)
- [15] Chang, Y.P., Tsai, R. and Sui, F.M., The effect of thermophoresis on particle deposition from a mixed convection flow onto a vertical flat plate, **J. Aerosol Sci.**, 30, 1363-1378 (1999).

- [16] Ahmadi, G. and He, C., Particle deposition with thermophoresis in a laminar duct flow and in a turbulent pipe flow with a sudden expansion, **1996 Annual Technical Meeting, Centre for Advanced Material Processing (CAMP), Lake Placid, New York, May 14-16** (1996).
- [17] Greenfield, C. and Quairini, G., A Lagrangian simulation of particle deposition in a turbulent boundary layer in the presence of thermophoresis, **Appl. Math. Model.**, 22, 10, 759-771 (1998).
- [18] Chamkha, A.J. and Pop, I., Effect of thermophoresis particle deposition in free convective boundary layer from a vertical flat plate embedded in porous medium, **Int. Comm. Heat Mass Transfer**, 31, 421-430 (2004).
- [19] Bég, O.A. and Takhar, H. S., Effects of transverse magnetic field, Prandtl number and Reynolds number on non-Darcy mixed convective flow of an incompressible viscous fluid past a porous vertical flat plate in saturated porous media, **Int. J. Energy Research**, 21, 87-100 (1997).
- [20] O. A. Bég, H.S. Takhar, G. Nath and M. Kumari, Computational fluid dynamics modeling of buoyancy-induced viscoelastic flow in a porous medium with magnetic field effects, **Int. J. Applied Mechanics and Engineering**, 6, 1, 187-210 (2001).
- [21] O. A. Bég, A. J. Chamkha and Takhar, H. S., Numerical modeling of Darcy-Brinkman-Forchheimer magneto hydro-dynamic mixed convection flow in a porous medium with transpiration and viscous (Eckert) heating, **Int. J. Fluid Mechanics Research**, 29, 1, 1-26 (2002).
- [22] Tynjala, T., Hajiloo, A., Polashenski, W. and Zamankhan, P., Magneto-dissipation in ferrofluids, **J. Magnetism and Magnetic Materials**, 252, 123-125 (2002).
- [23] O. A. Bég, A. K. Singh and H S. Takhar Multi-parameter perturbation analysis of unsteady, oscillatory, magneto-convection in porous media with heat source effects, **Int. J. Fluid Mechanics Research**, 32, 6, 635-661 (2005).
- [24] Zueco, J., Numerical study of an unsteady free convective magnetohydrodynamic flow of a dissipative fluid along a vertical plate subject to a constant heat flux, **Int. J. Engineering Science**, 44, 1380-1393 (2006).
- [25] O. A. Bég, H. S. Takhar, G. Nath and A. J. Chamkha, Mathematical Modeling of hydromagnetic convection from a rotating sphere with impulsive motion and buoyancy effects, **Non-Linear Analysis: Modeling and Control J.**, 11, 3, 1-19 (2006).

- [26] R. Bhargava, S. Rawat, H.S. Takhar and O. A. Bég, Finite element modeling of pulsatile magneto-biofluid flow and dispersion in a channel, **Mecannica J.**, 42, 4, 37-52 (2007).
- [27] H. Naroua, H.S. Takhar, P.C. Ram, Tasveer A. Bég and O. Anwar Bég, Rotating Hydromagnetic Transient Partially-Ionized Heat-Generating Gas Dynamic Flow with Hall/Ion Slip Current Effects: Finite Element Analysis, **Int. J. Fluid Mech Research**, (2007) [in press].
- [28] Chamkha, A.J. and Camille, I., Effects of heat generation/absorption and thermophoresis on hydromagnetic flow with heat and mass transfer over a flat surface, **Int. J. Numerical Methods in Heat and Fluid Flow**, 10, 432-448 (2000).
- [29] Zueco J., Campo A., Transient radiative transfer between the thick walls of an enclosure using the network simulation method, **Applied Thermal Engineering**, 26, 673-679 (2006).
- [30] Zueco, J., A network thermodynamic method for the numerical solution of Burgers' equation, **Mathematical and Computation Modelling** (in press).
- [31] Zueco, J., Unsteady free convection- radiation flow over a vertical wall embedded in a porous medium, **Commun. Numer. Method Engineering**, (in press).
- [32] Zueco, J. and Bég, O.A., Numerical Network simulation of electrohydrodynamics of ion drag flow in a dc unipolar pump with electrical Reynolds number, electrical slip and electrical source effects, **International Journal of Applied Mathematics and Mechanics**, submitted, January (2009).
- [33] **Pspice 6.0.** Irvine, California 92718. Microsim Corporation, 20 Fairbanks (1994).
- [34] White, F.M., **Viscous Fluid Flow**, 1st edition, MacGraw-Hill, New York (1974).
- [35] Schlichting, H., **Boundary-Layer Theory**, 7<sup>th</sup> edition, MacGraw-Hill, New York (1979).
- [36] Chamkha, A.J., Mudhaf-Al, A.F. and Pop, I., Effect of heat generation or absorption in thermophoretic free convection boundary layer from a vertical flat plate embedded in a porous medium, **Int. Comm. Heat Mass Transfer**, 33, 1096-1102 (2006).
- [37] Tsai, R., A simple approach for evaluating the effect of wall suction and thermophoresis on aerosol particle deposition from a laminar flow over a flat plate, **Int. Comm. Heat Mass Transfer**, 26, 249-257 (1999).
-

- [38] Hsu, F.K. and Grief, R., Stagnation flow of thermophoretic deposition with variable particle concentration in the mainstream, **Int. J. Heat Mass Transfer**, 45, 1229-1235 (2002).
- [39] Blums, E. and Odenbach, S., Thermophoretic separation of ultrafine particles in ferrofluids in thermal diffusion column under the effect of an MHD convection, **Int. J. Heat Mass Transfer**, 43, 1637-1649 (2000).
- [40] Blums, E., Mezulis, A., Mairov, M. and Kronkalns, G., Thermal diffusion of magnetic nanoparticles in ferrocolloids: experiments on particle separation in vertical columns, **J. Magnetism and Magnetic Materials**, 169, 220-228 (1997).
- [41] Zahmatkesh, I., On the importance of thermophoresis and Brownian diffusion for the deposition of micro-and nano-particles, **Int. Communications Heat Mass Transfer**, 35, 369-375 (2008).
- [42] Bacri, J-C., Cebers, A., Bourdon, A., Demouchy, G., Heegard, B.M., Kashevsky, B.M. and Perzynski, R., Transient grating in a ferrofluid under magnetic field: effect of magnetic interactions on the diffusion coefficient of translation, **Physics Review E**: 52, 3936-3942 (1995).

## 7. ACKNOWLEDGEMENTS

The authors are very grateful to the reviewer for his comments which have served to improve the paper.

---